

# Dominance of Exciton Lifetime in the Stability of Phosphorescent Dyes

Dong-Gwang Ha<sup>1†</sup>, Jan Tiepelt<sup>2†</sup>, Michael A. Fusella<sup>3</sup>, Michael S. Weaver<sup>3</sup>, Julie Brown<sup>3</sup>, Markus Einzinger<sup>2</sup>, Michelle Sherrott<sup>2</sup>, Troy Van Voorhis<sup>4</sup>, Nicholas J. Thompson<sup>3</sup>, and Marc A. Baldo<sup>2</sup>

<sup>1</sup> Department of Materials Science and Engineering, Massachusetts Institute of Technology, 77 Massachusetts Avenue, Cambridge, MA 02139 USA

<sup>2</sup> Department of Electrical Engineering and Computer Science, Massachusetts Institute of Technology, 77 Massachusetts Avenue, Cambridge, MA 02139 USA

<sup>3</sup> Universal Display Corporation, 375 Phillips Boulevard, Ewing, New Jersey 08618, USA

<sup>4</sup> Department of Chemistry, Massachusetts Institute of Technology, 77 Massachusetts Avenue, Cambridge, MA 02139 USA

<sup>†</sup>These authors contributed equally to this work

## Abstract

Organic light-emitting devices (OLEDs) are widely used for mobile displays, but the relatively short lifetime of blue OLEDs remains a challenge in many applications. Typically, instability is viewed as a material-specific chemical degradation problem. It is known to be alleviated by reducing the operating current or otherwise decreasing the exciton density. We show here that this view is incomplete. For archetypical phosphorescent materials, we observe that the dependence of photostability on the triplet exciton lifetime follows a *cubic* power law, steeper than its dependence on exciton density. We demonstrate that the triplet exciton lifetime not only determines the energy stored within an OLED, it also determines the loss in luminescence by controlling the yield of quenching by defects. The dominant role of the triplet exciton lifetime suggests that the stability of the best OLED materials can be significantly improved via rapid extraction of the energy stored in triplet excitons.

This is the author manuscript accepted for publication and has undergone full peer review but has not been through the copyediting, typesetting, pagination and proofreading process, which may lead to differences between this version and the [Version of Record](#). Please cite this article as [doi: 10.1002/adom.201901048](#).

OLEDs are presently the leading display technology for mobile devices, with growing applications in televisions and solid-state lighting. Amidst this success, perhaps the greatest remaining challenge is to resolve the poor stability of high-efficiency blue OLEDs. Phosphorescent dyes<sup>[1,2]</sup>, which emit from the usually non-radiative triplet state, are the leading commercial high-efficiency technology in red and green, but blue phosphorescent devices degrade to 90% of their initial luminance within 150 hours continuous operation at 1000 nits<sup>[3]</sup>.

Many efforts have been made to understand OLED degradation behavior<sup>[3–6],[7–10]</sup>. While extrinsic degradation mechanisms have been identified and minimized<sup>[11]</sup>, routine identification of primary intrinsic degradation mechanisms has not been developed. Indeed, diagnostic spectroscopy at the microscopic level is challenging given the exceedingly rare processes involved. Red phosphorescent OLEDs, for example, exhibit a decay time to 95% of initial luminance (*LT95*) of ~20,000 hours at an operating brightness of 1000 nits<sup>[12]</sup>. Given that the active phosphorescent dye is present at 3% loading in a 30-nm-thick emissive layer, this yields more than 60 *billion* excitons per dye to *LT90*. One approach to the experimental challenge is to build models that consider an array of possible phenomena that are then fit to degradation data for a specific combination of materials in a specific device structure<sup>[3,4,13–18]</sup>. Due to the multitude of fitting parameters, however, such models do not allow for an unequivocal, and more importantly, generalized quantification of physical parameters governing degradation.

Given the challenges that confront the rational design of OLED materials, it is important to determine general characteristics of OLED failure processes by isolating individual key parameters in direct experimental probes. We focus on long-lived triplet excitons, which are common to all OLEDs, and are hypothesized as an important energy source for degradation processes. The total energy stored in triplet excitons is dependent on

the triplet exciton density which, in turn, is determined by the triplet exciton generation rate,  $G$ , and the triplet exciton lifetime,  $\tau$ . Using these two key parameters, we construct a simple model of OLED degradation based on three primary classes of known failure mechanisms.

As shown in Table 1, the first class (*i*) of degradation mechanisms is unimolecular pathways. Examples include spontaneous degradation of a given molecule in its excited state, or an impurity-assisted process such as photo-oxidation<sup>[19]</sup>. Unimolecular processes are distinguished from the other classes because they scale linearly with the number of triplet excited states in the OLED. The second class (*ii*) of degradation mechanism is triplet-charge interactions<sup>[14,20]</sup>. Here, triplet excitons collide with a charged molecule, forming a high energy state which initiates permanent damage to one of the molecules. Assuming that the charge density is determined by non-geminate recombination, these processes are expected to scale as the excitation intensity to the power of 1.5<sup>[21]</sup>. The final class (*iii*) of degradation mechanism is triplet-triplet interactions<sup>[3]</sup>. Here, two triplet excitons collide, forming a high energy state leading to permanent damage to a molecule. These processes scale quadratically with the number of excited states in the OLED<sup>[22]</sup>.

Conceptually, we can understand degradation in terms of the energy density stored in the device; the energy density depends equally on the generation rate and the triplet exciton lifetime. This simple analysis suggests that changes to the triplet exciton lifetime should be roughly equivalent to changes in an OLED's luminance. Once formed, however, a damaged molecular site may quench neighboring molecules, thereby amplifying the impact on an OLED's performance<sup>[18,23,24]</sup>. While the yield of exciton quenching at non-luminescent defects is independent of the exciton generation rate, it *is* dependent on the triplet exciton lifetime. Indeed, quenching is the crucial phenomenon that increases the dependence of emitter stability on the triplet lifetime relative to its dependence on the exciton generation

rate. The expected dependence of each class of degradation mechanism on the overall triplet exciton lifetime  $\tau$ , and the triplet exciton generation rate  $G$  is:

$$1/LT90 \propto G\tau^2 \quad (i), \quad 1/LT90 \propto G^{1.5}\tau^2 \quad (ii), \quad 1/LT90 \propto G^2\tau^3 \quad (iii) \quad \#(1)$$

where the solutions for unimolecular, triplet-charge, and triplet-triplet cases are marked (i), (ii), and (iii), respectively.  $LT90$  is the time required for the OLED to degrade to 90% of initial luminance. The same dependencies are expected for  $LT97$  and  $LT95$ , but in this study we measure  $LT90$ . See Supplementary Note 1 for a detailed derivation of Eq. 1.

As argued conceptually above, Equation 1 predicts that, in each case, the dependence of stability on triplet exciton lifetime is dramatic, stronger even than the dependence on generation rate. To test the predictions for triplet-triplet and triplet-charge induced degradation, while keeping the exciton generation rate constant, we systematically reduce the triplet exciton lifetime by engineering a competing decay into surface plasmon modes.

Experimentally, we consider optically pumped films of green and blue Ir-based phosphorescent dyes. Notably, this allows us to isolate the key parameter,  $\tau$ , while leaving all other experimental parameters such as emissive layer thickness and composition unchanged. The green emitter is the well-studied phosphorescent dye *fac*-tris(2-phenylpyridine) Iridium(III) ( $\text{Ir(ppy)}_3$ ). It is employed as a neat film, where it exhibits strong triplet-triplet annihilation<sup>[25]</sup>, sandwiched by the host material 4,4'-bis(N-carbazolyl)-1,1'-biphenyl (CBP). The second material is *fac*-tris[3-(2,6-dimethylphenyl)-7-methylimidazo(1,2-f)phenanthridine] Iridium(III) ( $\text{Ir(dmp)}_3$ ) doped at 10% by volume into 3,3'-bis(N-methylcarbazolyl)-1,1'-biphenyl (mCBP) sandwiched by the host material mCBP. The lowest unoccupied molecular orbital (LUMO) of mCBP is near in energy to the LUMO of  $\text{Ir(dmp)}_3$  such that free charge is generated under optical excitation of the system. The degradation behavior of this system is dominated by triplet-charge interactions<sup>[4]</sup>. The chemical structures and energy levels of these materials are shown in Fig. 1a and 1b.

To control the exciton lifetime of the phosphorescent dyes, we deposit them on films of Ag with a host material spacer layer of variable thickness,  $d$ . As shown in Fig. 1c and 1d, this approach exploits the well-known phenomenon of non-radiative energy transfer to surface plasmon polaritons in the Ag film<sup>[26–28]</sup>. The combination of the guest-host systems of varying concentration at a tunable spacer layer distance from an adjacent silver film allows us to systematically vary the degradation mechanism and triplet exciton lifetime, without the need to chemically modify the materials to do so.

The transient photoluminescence (PL) responses for varying spacer thicknesses are shown in Fig. 2a and 2b. To determine the impact of triplet exciton lifetime on stability, we measure the photostability of the samples under continuous excitation by a  $\lambda = 405$  nm laser; see Fig. 2c and 2d. See Supplementary Note 2 for details of the data processing. As predicted by Equation 1, we find that the films with longer triplet exciton lifetimes degrade faster. For each film we extract the time required for the PL intensity to fall to 90% of its initial value ( $LT90$ ). Care is taken to ensure that the optical generation rate of triplet excitons is identical for all films. The pump power is corrected based on transfer-matrix calculation of absorption<sup>[29]</sup> and in accordance with experimentally determined pump-power dependencies for each sample. The calculated absorption is verified by direct measurement of absorption in an integrating sphere; see Supplementary Note 3.

Using the data in Fig. 2, we extract the measured dependence of phosphorescent dye stability on the triplet exciton lifetime,  $\tau$ . We summarize these results in Fig. 3 where we show the degradation behaviors of both 10% Ir(dmp)<sub>3</sub>:mCBP and neat Ir(ppy)<sub>3</sub>. The dependence of stability for each system on  $\tau$  is substantial, as predicted by Eq. 1. The stability of 10% Ir(dmp)<sub>3</sub>:mCBP, which is dominated by triplet-charge interactions, exhibits a power law dependence on  $\tau$  with an exponent of 2.9. For neat Ir(ppy)<sub>3</sub>, dominated by triplet-triplet degradation events, the power law dependence of stability on  $\tau$  is 3.6. A seven-fold reduction

in exciton lifetime thus leads to a *1000-fold* improvement in the photostability of neat Ir(ppy)<sub>3</sub>. We note that all of the measured power law dependencies on  $\tau$  are larger than the predictions in Eq. 1. For the doped system, which generates charge, the discrepancy could be partially due to the dissociation of triplet excitons into charge which yields  $1/LT90 \propto \tau^{2.5}$ ; see Supplementary Note 1. The systematically steeper slopes may also suggest that additional triplet dynamics play a role in the quenching process. For example, the contribution of triplet exciton diffusion to the quenching process can induce additional dependence on exciton lifetime; see Supplementary Note 1. The experimental data nevertheless confirm that the simple model of Eq. 1 provides a conservative estimate for the potential stability improvements achievable with changes in triplet lifetime.

In Supplementary Note 4, we also characterize neat Ir(dmp)<sub>3</sub>, which exhibited green excimer emission and was not studied further, and 10% Ir(ppy)<sub>3</sub>:CBP, which was found to behave similarly to 10% Ir(dmp)<sub>3</sub>:mCBP. Similar to Ir(dmp)<sub>3</sub>:mCBP, where electron and hole transport occurs preferentially on the host and guest, respectively<sup>[4]</sup>, the Ir(ppy)<sub>3</sub>:CBP system can separate charge under photoexcitation. This is confirmed experimentally; see Supplementary Note 5. The charging is exacerbated in the vicinity of the silver film, where it is characterized by the onset of delayed luminescence in the transient PL. The presence of multiple distinct lifetimes and the evidence of additional dynamics close to the silver causes us to neglect samples characterized by strong delayed luminescence; see Supplementary Note 6.

The dependence of photodegradation on the triplet exciton generation rate,  $G$ , offers an additional test of the predictions in Eq. 1. The relevant data for neat Ir(ppy)<sub>3</sub> and 10% Ir(dmp)<sub>3</sub>:mCBP is shown in Fig. 3, and the pump-power dependence of 10% Ir(ppy)<sub>3</sub>:CBP is described in Supplementary Note 7. The results are consistent with expectations<sup>[21],[22]</sup> for triplet-charge and triplet-triplet induced degradation in the doped systems and neat Ir(ppy)<sub>3</sub>,

respectively. We find that the power law governing the dependence of pump intensity has a slope of approximately 1.5 for the 10% doped systems and 2.0 for neat Ir(ppy)<sub>3</sub>, as predicted by Eq. 1(ii) and 1(iii), respectively. Interestingly, doped Ir(ppy)<sub>3</sub> in the absence of a silver film and doped Ir(dmp)<sub>3</sub> with large separation of 150 nm between the emission layer and the silver film yield power law slopes of approximately 1. In both cases, the apparent charging in the materials is reduced, yielding unimolecular power law dependencies. We note that these systems are unlikely to be relevant to OLEDs, given the substantial densities of charge expected in OLEDs under bias. We also characterize photodegradation as a function of the Ir(ppy)<sub>3</sub> doping ratio in CBP films, observing the expected transition to triplet-triplet interactions at high doping densities; see Supplementary Note 7.

Considering these results in the context of modern OLEDs, we note that the observed dependence of stability on the triplet exciton lifetime should motivate the development of new device designs that apply Purcell enhancements to phosphorescent dyes, which are unique in that their long-lived states are radiative. OLEDs with high brightness and enhanced stability could be realized by rapidly extracting energy via coupling to surface plasmons, combined with an optical outcoupling mechanism to radiate the energy back into free space. Faster triplet exciton lifetimes also promise to reduce efficiency droop at high excitation densities<sup>[22,30]</sup>, a key secondary challenge for future OLED applications. The potential improvement to droop can be quantified using the experimental probes developed here to study stability.

To summarize, OLEDs store energy in excited states during the conversion of injected charge into light. Reducing the stored energy density by expanding the exciton recombination zone or lowering the current density is known to alleviate degradation processes<sup>[3–6]</sup>. The triplet exciton lifetime is the other crucial determinant of the stored energy density, and it additionally controls the yield of luminescence quenching by defects. By experimentally

isolating this key parameter, we observe that it dominates the photostability of phosphorescent dyes. We measure a *cubic* dependence of stability on the exciton lifetime. Indeed, a 7-fold change in triplet exciton lifetime yields up to a *1000-fold* improvement in photostability. If the triplet exciton lifetime can be engineered without incurring major non-radiative loss, the potential improvement is more than enough to stabilize phosphorescent blue materials for many applications.

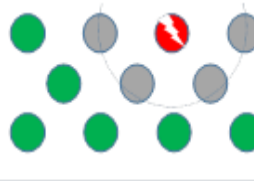
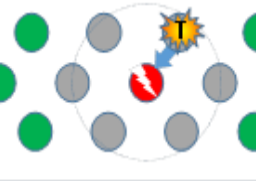

## Methods

Photoluminescent samples were grown via vacuum thermal evaporation. Prior to any organic layer deposition or coating, the soda-lime glass substrate was degreased with solvents, dried, and then treated with oxygen plasma for 1.5 minutes and ultra violet ozone for 5 minutes. The samples were fabricated in high vacuum ( $< 10^{-6}$  Torr). The Ag layer was fabricated on a 10 Å thick Aluminum adhesion layer followed by the specified thickness of Ag. All layers were grown at a rate of either 1 or 2 Å/s. All samples were encapsulated with a glass lid and sealed with an ultra violet cured epoxy in a nitrogen glove box ( $< 1$  ppm of  $H_2O$  and  $O_2$ ) immediately after fabrication. For doped layers, doping percentages are in volume percent. All samples were prepared at Universal Display Corporation.

Ellipsometry data was measured with a J.A. Woollam RC2 variable angle ellipsometer. To accurately determine the optical constants and thicknesses of the metal layers, thin layers of the metal were grown on a Si wafer with a  $\sim 1500$  Å thermal oxide.

For the photodegradation measurement, a  $\lambda = 405$  nm laser (CPS405, Thorlabs) was used as the excitation source. The excitation power deviation was tracked with a 90:10 beam splitter and a silicon photodetector (818-SL, Newport). A  $\lambda = 450$  nm short pass filter was used for the excitation power detection. Another silicon photodetector was used for PL detection with a  $\lambda = 450$  nm longpass filter and a  $\lambda = 700$  nm shortpass filter. The

photodetectors were connected to two lock-in amplifiers (SR830, Stanford Research Systems) to reduce measurement noise. The sample was excited at 45-degree angle and detection optics were placed to normal direction. All measurements were done in an optical enclosure. Transient PL was measured with a streak camera (Hamamatsu C11200 and a  $\lambda=371$  nm laser diode).

Defect generation mechanism	(i) Unimolecular process	(ii) Triplet-Charge Interaction	(iii) Triplet-Triplet Interaction
Defect generation rate	$\propto G\tau$	$\propto G^{1.5}\tau$	$\propto G^2\tau^2$
Excitons quenched by defects			
Quenching loss	$\propto \tau$		
$1/LT90$	$\propto G\tau^2$	$\propto G^{1.5}\tau^2$	$\propto G^2\tau^3$

**Table 1.** The three classes of degradation mechanisms that generate defects within an OLED and their defect generation rate as a function of triplet exciton-generation rate ( $G$ ) and triplet exciton lifetime ( $\tau$ ). The dependence of the OLED lifetime to 90% of initial lifetime ( $LT90$ ) on the triplet exciton lifetime is significant because  $\tau$  not only contributes to the triplet exciton density, but also influences quenching losses at defect sites. The details of the derivation are in Supplementary Note 1.

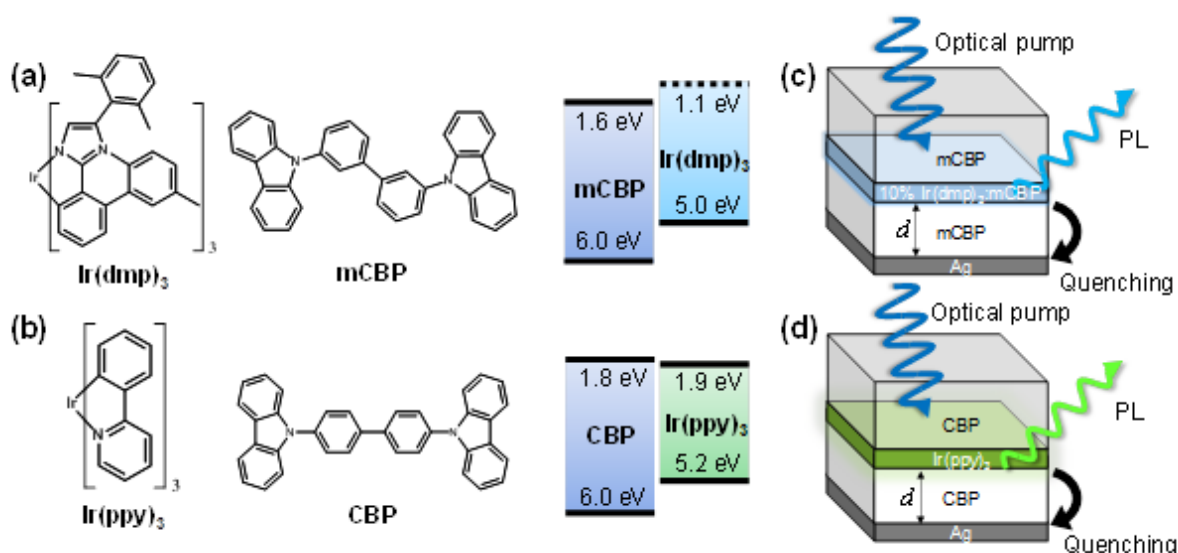


**Figure 1.** The chemical structures and energy levels of (a) blue, and (b) green material combinations. The energy levels of the highest occupied molecular orbitals were determined by photoemission spectroscopy for  $\text{Ir(ppy)}_3$ ,  $\text{CBP}$ ,  $\text{Ir(dmp)}_3$ , and  $\text{mCBP}$ <sup>[4,31,32]</sup>. The lowest unoccupied molecular orbitals of  $\text{Ir(ppy)}_3$ ,  $\text{CBP}$  and  $\text{mCBP}$  were determined by inverse photoemission spectroscopy<sup>[31,32]</sup>. The lowest unoccupied molecular orbital level of  $\text{Ir(dmp)}_3$  was determined from the optical gap and assuming identical exciton binding energy of  $\text{Ir(ppy)}_3$ . The sample structure for the blue system (c) is  $\text{Ag}(34 \text{ nm})/\text{mCBP}(10, 20, 45, 150 \text{ nm})/\text{Emission layer}(10 \text{ nm})/\text{mCBP}(10 \text{ nm})$  and the green system (d) is  $\text{Ag}(20 \text{ nm})/\text{CBP}(0, 5, 10, 20, 45, 100 \text{ nm})/\text{Emission layer}(10 \text{ nm})/\text{CBP}(10 \text{ nm})$ .

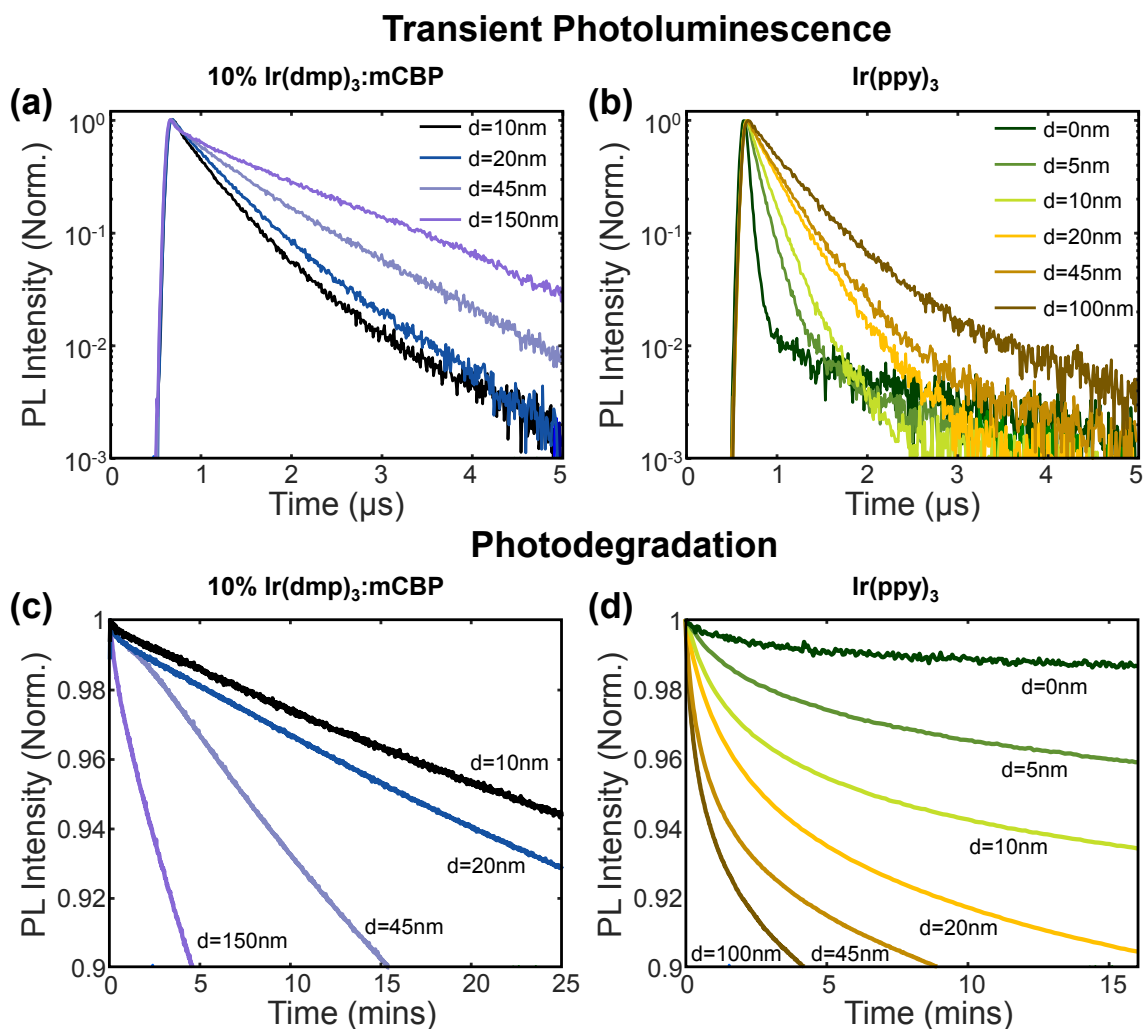


**Figure 2.** Transient PL decay of **(a)** 10% Ir(dmp)<sub>3</sub>:mCBP and **(b)** neat Ir(ppy)<sub>3</sub>, as a function of varying spacer thickness  $d$ . As expected, reducing the distance between the emission layer and the Ag corresponds to increasingly fast exciton decay due to strong coupling to the non-radiative surface plasmonic modes in Ag. The PL degradation curves for the **(c)** blue and **(d)** green systems as a function of  $d$ . Samples with emission layers closer to Ag experience a stabilizing effect, *i.e.* slower PL degradation. The data for doped Ir(ppy)<sub>3</sub> samples are shown in Supplementary Fig. 3 and 4.

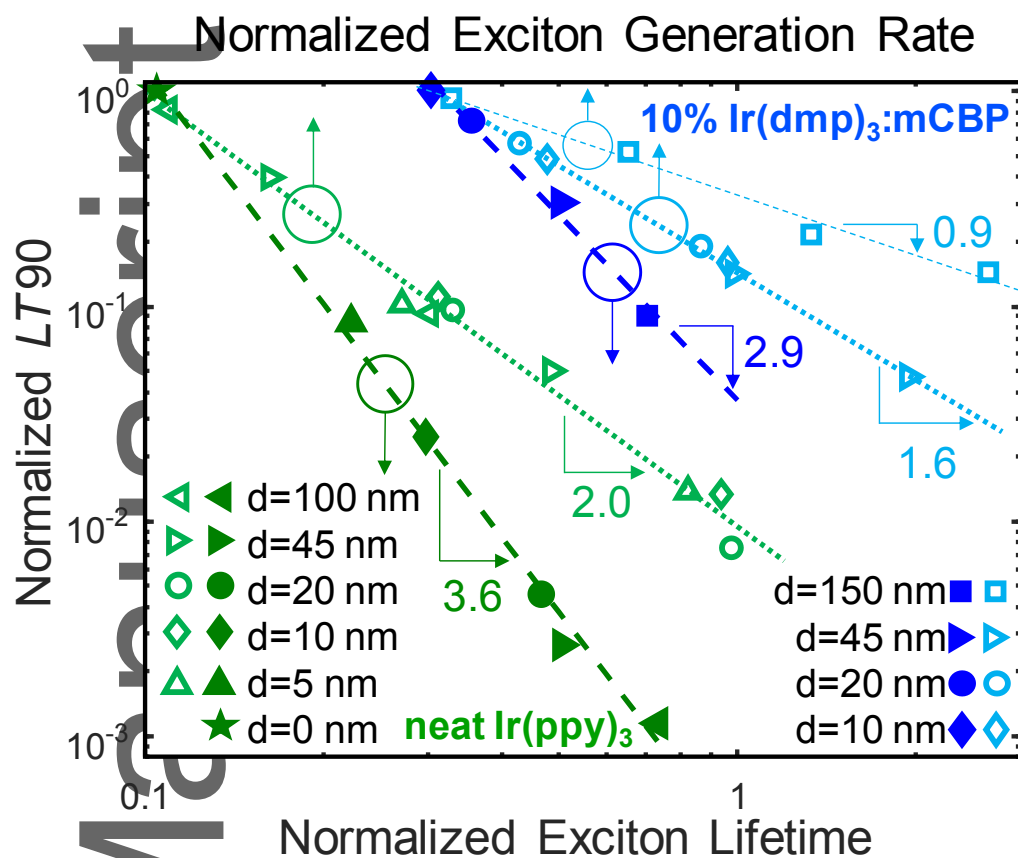


**Figure 3.** The stability in both green and blue systems as a function of the generation rate of triplet excitons,  $G$ , and the triplet exciton lifetime,  $\tau$ . Differing symbols correspond to the values of  $d$  used to obtain each data point. Values for  $LT90$  are extracted from the data presented in Fig. 2 and plotted on a normalized logarithmic scale against (top) triplet exciton generation rate ( $G$ ) and (bottom) triplet exciton lifetime ( $\tau$ ). See Supplementary Note 2 for details on the normalization of data points plotted against exciton generation rate.

## References

- [1] M. A. Baldo, D. F. O'Brien, Y. You, A. Shoustikov, S. Sibley, M. E. Thompson, S. R. Forrest, *Nature* **1998**, *395*, 151.
- [2] M. A. Baldo, S. Lamansky, P. E. Burrows, M. E. Thompson, S. R. Forrest, *Appl. Phys. Lett.* **1999**, *75*, 4.
- [3] J. Lee, C. Jeong, T. Batagoda, C. Coburn, M. E. Thompson, S. R. Forrest, *Nat. Commun.* **2017**, *8*, 15566.
- [4] Y. Zhang, J. Lee, S. R. Forrest, *Nat. Commun.* **2014**, *5*, 5008.
- [5] D. P. K. Tsang, C. Adachi, *Sci. Rep.* **2016**, *6*, 1.
- [6] J. M. Kim, C. H. Lee, J. J. Kim, *Appl. Phys. Lett.* **2017**, *111*, 1.
- [7] S. Scholz, D. Kondakov, B. Lüssem, K. Leo, *Chem. Rev.* **2015**, *115*, 8449.
- [8] S. Schmidbauer, A. Hohenleutner, B. König, *Adv. Mater.* **2013**, *25*, 2114.
- [9] F. So, D. Kondakov, *Adv. Mater.* **2010**, *22*, 3762.
- [10] H. Aziz, Z. D. Popovic, *Chem. Mater.* **2004**, *16*, 4522.
- [11] H. Yamamoto, C. Adachi, M. S. Weaver, J. J. Brown, *Appl. Phys. Lett.* **2012**, *100*, 183306.
- [12] X. Xu, V. Adamovich, B. Ma, A. Deangelis, S. Xia, M. S. Weaver, J. J. Brown, *SID Int. Symp. Dig. Tech. Pap.* **2012**, 614.
- [13] C. Fry, B. Racine, D. Vaufrey, H. Doyeux, S. Cih, *Appl. Phys. Lett.* **2005**, *87*, 213502.
- [14] N. C. Giebink, B. W. D'Andrade, M. S. Weaver, P. B. MacKenzie, J. J. Brown, M. E. Thompson, S. R. Forrest, *J. Appl. Phys.* **2008**, *103*, DOI 10.1063/1.2884530.
- [15] D. Y. Kondakov, *Org. Electron. Mater. Process. Devices Appl.* **2010**, 211.
- [16] P. N. Marques dos Anjos, *J. Inf. Disp.* **2013**, *14*, 115.
- [17] R. Coehoorn, H. Van Eersel, P. A. Bobbert, R. A. J. Janssen, *Adv. Funct. Mater.* **2015**, *25*, 2024.

- [18] T. D. Schmidt, L. Jäger, Y. Noguchi, H. Ishii, W. Brütting, *J. Appl. Phys.* **2015**, *117*, DOI 10.1063/1.4921829.
- [19] M. Murgia, R. H. Michel, G. Ruani, W. Gebauer, O. Kapousta, R. Zamboni, C. Taliani, *Synth. Met.* **1999**, *102*, 1095.
- [20] N. C. Giebink, B. W. D'Andrade, M. S. Weaver, J. J. Brown, S. R. Forrest, *J. Appl. Phys.* **2009**, *105*, DOI 10.1063/1.3151689.
- [21] S. Reineke, K. Walzer, K. Leo, *Phys. Rev. B* **2007**, *75*, 125328.
- [22] M. A. Baldo, C. Adachi, S. R. Forrest, *Phys. Rev. B* **2000**, *62*, 10967.
- [23] Z. D. Popovic, H. Aziz, N. X. Hu, A. Ioannidis, P. N. M. Dos Anjos, *J. Appl. Phys.* **2001**, *89*, 4673.
- [24] T. D. Schmidt, D. S. Setz, M. Flämmich, B. J. Scholz, A. Jaeger, C. Diez, D. Michaelis, N. Danz, W. Brütting, *Appl. Phys. Lett.* **2012**, *101*, 103301.
- [25] W. Holzer, A. Penzkofer, T. Tsuboi, *Chem. Phys.* **2005**, *308*, 93.
- [26] K. Celebi, T. D. Heidel, M. A. Baldo, *Opt. Express* **2007**, *15*, 1762.
- [27] S. Paquette, Enhanced Photostability In Organic Thin Films Deposited On Plasmonic Substrates, University of Rochester, **2012**.
- [28] Catrice Carter; Zeqing Shen; Kun Zhu; Kelsey Gwynne; Deirdre M. O'Carroll, in *Proc. SPIE 10529, Org. Photonic Mater. Devices XX*, **2018**, p. 1052907.
- [29] L. A. A. Pettersson, L. S. Roman, O. Inganäs, *J. Appl. Phys.* **1999**, *86*, 487.
- [30] M. Einzinger, T. Zhu, P. de Silva, C. Belger, T. M. Swager, T. Van Voorhis, M. A. Baldo, *Adv. Mater.* **2017**, *29*, 1.
- [31] H. Yoshida, K. Yoshizaki, *Org. Electron.* **2015**, *20*, 24.
- [32] T. Matsushima, C. Qin, K. Goushi, F. Bencheikh, T. Komino, M. Leyden, A. S. D. Sandanayaka, C. Adachi, *Adv. Mater.* **2018**, *30*, 1.

## **Acknowledgements**

Work at MIT was supported by the US Department of Energy, Office of Basic Energy Sciences (Award No. DE-FG02-07ER46474).

## **Author contributions**

M.A.B., J.T., N.T., and M.S.W. conceived the project. M.A.B. and D.-G.H. developed the theoretical model. N.J.T., M.A.F. and M.S.W. prepared the samples and measured refractive index of materials. D.-G.H. and J.T. measured absorption, transient PL and photodegradation. D.-G.H. performed the transfer-matrix calculation. M.E. and M.S. contributed to analysis. All authors discussed the results and commented on the manuscript.

## **Competing financial interests**

The authors at Universal Display Corporation declare the following competing interests: personal financial interests via UDC stock ownership, employment at UDC, and numerous granted and pending patent applications on phosphorescent emitters and OLED devices.

## **Materials & Correspondence**

Correspondence to Marc Baldo and Nicholas Thompson

Text for Table of contents

To understand the stability of organic light-emitting devices (OLEDs), the exciton lifetime is experimentally isolated and systematically varied. A 7-fold change in triplet exciton lifetime yields up to a 1000-fold improvement in photostability. The exciton lifetime plays a dominant role by controlling the yield of quenching by defects as well as the energy stored within an OLED.

